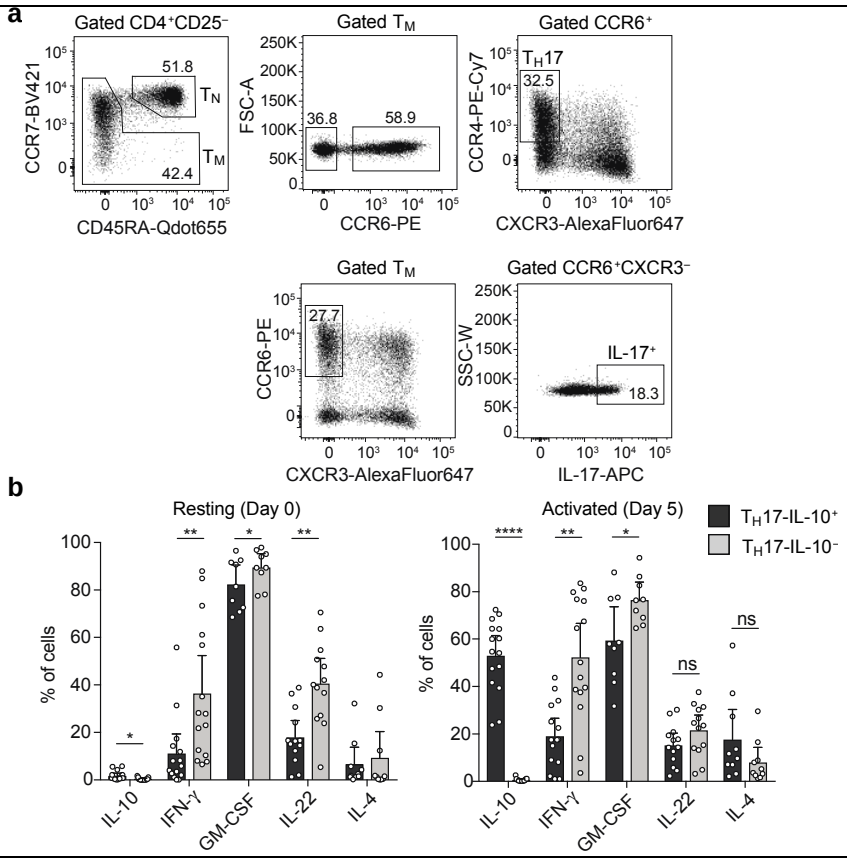

Supplementary Figure 1

Sorting strategy and cytokine production by subsets of human memory T_H17 cells

a. Sorting of human memory T_H17 cells from PBMCs based on chemokine receptor expression or cytokine secretion. MACS-enriched $CD4^+$ T cells were stained with antibodies to CD45RA, CD25, CCR7, CCR6, CCR4 and CXCR3. $CD4^+$ memory T_H17 cells were sorted, after exclusion of $CD45RA^+CCR7^+$ naïve T cells (T_N) and $CD8^+$ $CD14^+$ $CD19^+$ $CD56^+$ $CD25^+$ cells, as $CCR6^+CCR4^+CXCR3^-$ or, alternatively, as $CCR6^+CXCR3^-IL\text{-}17A^+$ (a, lower panels). Dot plots from one donor, representative of more than 10 donors analyzed. **b.** Cytokine production as assessed by intracellular staining in Day 0-resting and Day 5-activated $T_H17\text{-}IL10^+$ and $T_H17\text{-}IL\text{-}10^-$ clone pools after 5 h stimulation with PMA plus Ionomycine. Data are represented as mean + 95% c.i., with each dot indicating a T cell clone pool from independent experiments ($n \geq 9$) (note: the number of clone pools is paired and the same in $T_H17\text{-}IL\text{-}10^+$ and $T_H17\text{-}IL\text{-}10^-$, but can vary for different cytokines (IL-10 and IFN-γ, n = 15; IL-22, n = 13; IL-4, n = 10; GM-CSF, n = 9). *P < 0.05; **P < 0.01; ****P < 0.0001, as determined by ratio paired *t* test.

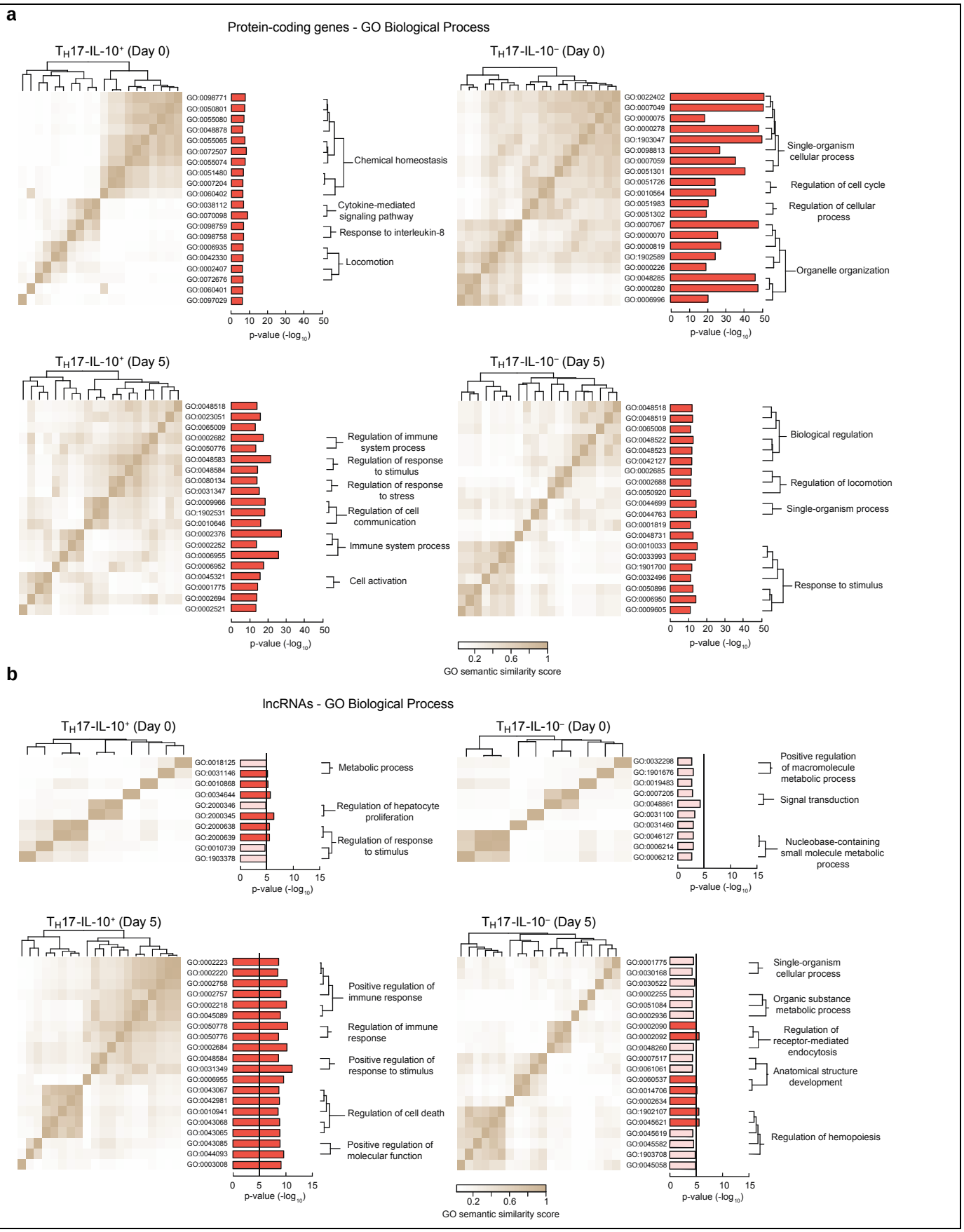
a
Protein-coding genes - GO Biological Process
TH17-IL-10+ (Day 0)
GO:0098771
GO:0050801
GO:0055080
GO:0048878
GO:0055065
GO:0072507
GO:0055074
GO:0051480
GO:0007204
GO:0060402
GO:0038112
GO:0070098
GO:0098759
GO:0098758
GO:0006935
GO:0042330
GO:0002407
GO:0072676
GO:0060401
GO:0097029
Chemical homeostasis
Cytokine-mediated signaling pathway
Response to interleukin-8
Locomotion
0 10 20 30 40 50
p-value (-log10)
TH17-IL-10− (Day 0)
GO:0022402
GO:0007049
GO:0000075
GO:0000278
GO:1903047
GO:0098813
GO:0007059
GO:0051301
GO:0051726
GO:0010564
GO:0051983
GO:0051302
GO:0007067
GO:0000070
GO:0000819
GO:1902589
GO:0000226
GO:0048285
GO:0000280
GO:0006996
Single-organism cellular process
Regulation of cell cycle
Regulation of cellular process
Organelle organization
0 10 20 30 40 50
p-value (-log10)
TH17-IL-10+ (Day 5)
GO:0048518
GO:0023051
GO:0065009
GO:0002682
GO:0050776
GO:0048583
GO:0048584
GO:0080134
GO:0031347
GO:0009966
GO:1902531
GO:0010646
GO:0002376
GO:0002252
GO:0006955
GO:0006952
GO:0045321
GO:0001775
GO:0002694
GO:0002521
Regulation of immune system process
Regulation of response to stimulus
Regulation of response to stress
Regulation of cell communication
Immune system process
Cell activation
0 10 20 30 40 50
p-value (-log10)
TH17-IL-10− (Day 5)
GO:0048518
GO:0048519
GO:0065008
GO:0048522
GO:0048523
GO:0042127
GO:0002685
GO:0002688
GO:0050920
GO:0044699
GO:0044763
GO:0001819
GO:0048731
GO:0010033
GO:0033993
GO:1901700
GO:0032496
GO:0050896
GO:0006950
GO:0009605
Biological regulation
Regulation of locomotion
Single-organism process
Response to stimulus
0 10 20 30 40 50
p-value (-log10)
0.2 0.6 1
GO semantic similarity score
b
lncRNAs - GO Biological Process
TH17-IL-10+ (Day 0)
GO:0018125
GO:0031146
GO:0010868
GO:0034644
GO:2000346
GO:2000345
GO:2000638
GO:2000639
GO:0010739
GO:1903378
Metabolic process
Regulation of hepatocyte proliferation
Regulation of response to stimulus
0 5 10 15
p-value (-log10)
TH17-IL-10− (Day 0)
GO:0032298
GO:1901676
GO:0019483
GO:0007205
GO:0048861
GO:0031100
GO:0031460
GO:0046127
GO:0006214
GO:0006212
Positive regulation of macromolecule metabolic process
Signal transduction
Nucleobase-containing small molecule metabolic process
0 5 10 15
p-value (-log10)
TH17-IL-10+ (Day 5)
GO:0002223
GO:0002220
GO:0002758
GO:0002757
GO:0002218
GO:0045089
GO:0050778
GO:0050776
GO:0002684
GO:0048584
GO:0031349
GO:0006955
GO:0043067
GO:0042981
GO:0010941
GO:0043068
GO:0043065
GO:0043085
GO:0044093
GO:0003008
Positive regulation of immune response
Regulation of immune response
Positive regulation of response to stimulus
Regulation of cell death
Positive regulation of molecular function
0 5 10 15
p-value (-log10)
TH17-IL-10− (Day 5)
GO:0001775
GO:0030168
GO:0030522
GO:0002255
GO:0051084
GO:0002936
GO:0002090
GO:0002092
GO:0048260
GO:0007517
GO:0061061
GO:0060537
GO:0014706
GO:0002634
GO:1902107
GO:0045621
GO:0045619
GO:0045582
GO:1903708
GO:0045058
Single-organism cellular process
Organic substance metabolic process
Regulation of receptor-mediated endocytosis
Anatomical structure development
Regulation of hemopoiesis
0 5 10 15
p-value (-log10)
0.2 0.6 1
GO semantic similarity score

Supplementary Figure 2
Gene ontology (GO) analyses of differentially expressed genes and lncRNAs in T_H17-IL-10^+ and T_H17-IL-10^- cells
Gene ontology (GO) analyses on the biological processes associated to the differentially expressed protein-coding genes (**a**) or lncRNAs (**b**) in Day 0-resting and Day 5-activated T_H17-IL-10^+ and T_H17-IL-10^- cells. GO terms are clustered by semantic similarity and a synthetic description is shown. *P*-value as determined by MetaCore based on hypergeometric distribution; *P*-value threshold (vertical line) set at 1×10^{-5}.

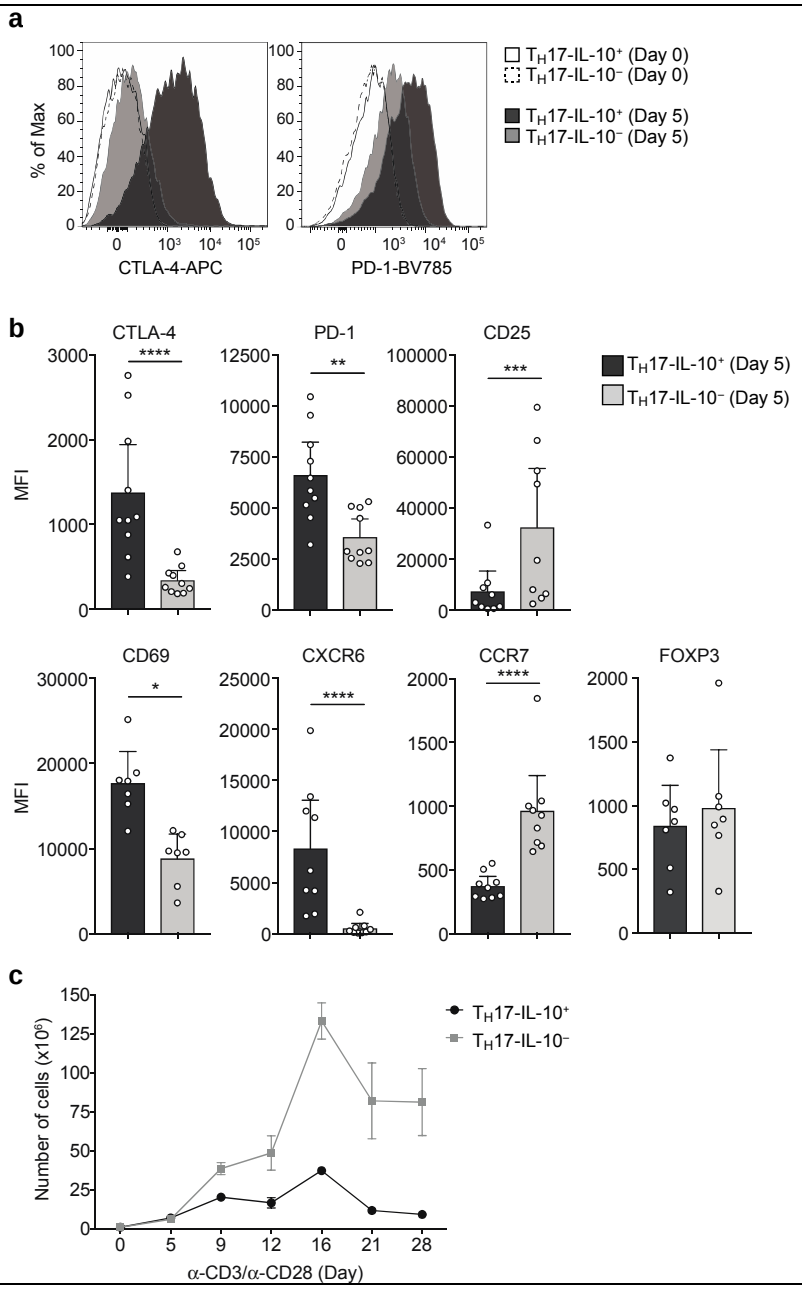

Supplementary Figure 3

Differential surface marker expression in T_H17-IL-10^+ and T_H17-IL-10^- cells

a,b. Expression of CTLA4, PD-1, CD25, CD69, CXCR6, CCR7 and FOXP3 as assessed by flow cytometry in Day 5-activated T_H17-IL-10^+ and T_H17-IL-10^- clone pools. Shown are representative histogram plots (**a**) and cumulative data of clone pools from independent experiments (mean + 95% c.i.; CTLA-4 and PD-1, n = 10; CD25, CXCR6 and CCR7, n = 9; CD69 and FOXP3, n = 7) (**b**). **P* < 0.05; ***P* < 0.01; ****P* < 0.001; *****P* < 0.0001, as determined by ratio paired *t* test. **c.** Expansion of T_H17-IL-10^+ and T_H17-IL-10^- cells in response to stimulation with CD3/CD28 antibodies. T_H17-IL-10^+ and T_H17-IL-10^- cells were stimulated with plate-bound CD3/CD28 antibodies for 48 h and their proliferation was measured at the indicated time points. Shown is the average of two independent experiments (mean ± s.e.m.).

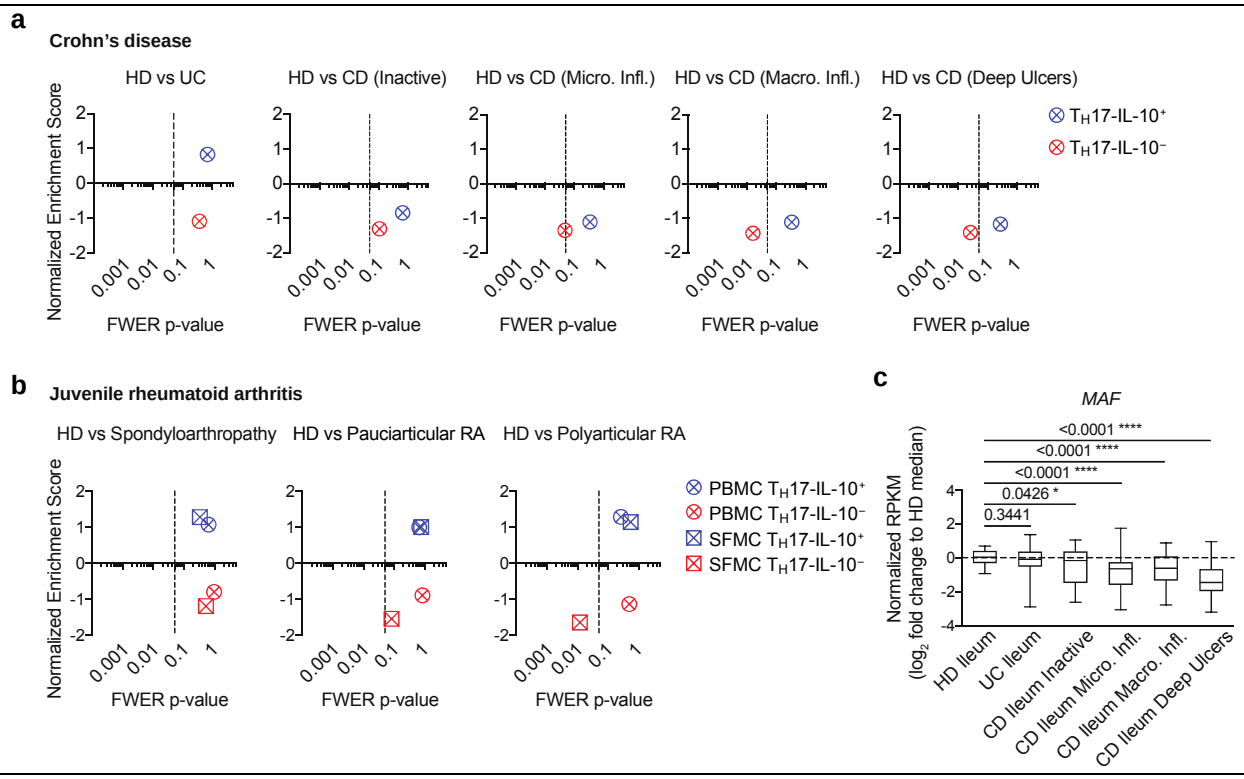

Supplementary Figure 4

Gene set enrichment analysis (GSEA) of T_H17-IL-10^+ and T_H17-IL-10^- transcriptional signatures in autoimmune diseases

Enrichment of T_H17-IL-10^+ and T_H17-IL-10^--associated gene signatures in publicly available transcriptional datasets of T_H17-mediated autoimmune diseases. Gene set enrichment in ileal biopsies from healthy donors (HD) vs. Crohn's patients (CD) (**a**) and in PBMC and SFMC from healthy donors (HD) vs. juvenile rheumatoid arthritis patients (RA) (**b**) are shown. GSEA enrichment results were reported as normalized enrichment score and familywise enrichment (FWER) *P* value. FWER *P* values smaller than 0.05 (dashed line) were considered significant. **c**. c-MAF expression in ileal biopsies from healthy donors (HD), ulcerative colitis (UC) and Crohn's disease (CD) patients, with histologically graded disease severity, is shown in a box (interquartiles, with a line indicating the median value) and whiskers (min to max values) plot. *P*-value as determined by Kruskal-Wallis test. Micro. Infl. = microscopic inflammation; Macro. Infl. = macroscopic inflammation.

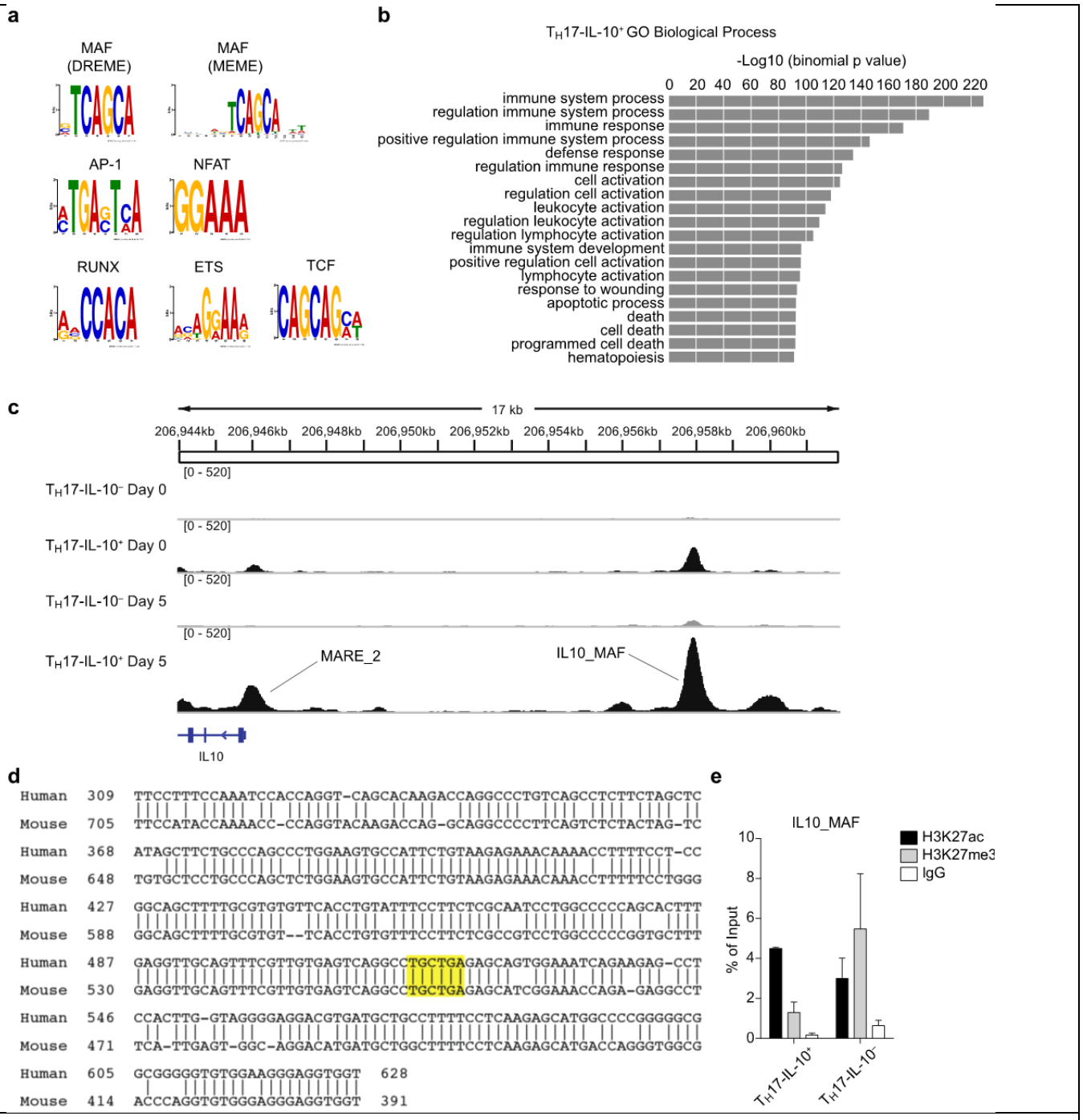

Supplementary Figure 5

c-MAF binds enhancer-like regions in proximity to genes involved in the immune response

a. Position weight matrix (PWM) of the top ranked DNA motives identified by the MEME suite software in the Day 5-activated T_H17-IL-10^+ c-MAF ChIP-seq dataset; *e*-values: MAF (DREME), 5.5 x 10^{-212}; MAF (MEME), 6.6 x 10^{-175}; AP-1, 1.7 x 10^{-146}; NFAT, 3.9 x 10^{-145}; RUNX, 2.6 x 10^{-81}; ETS, 1.1 x 10^{-57}; TCF, 1.1 x 10^{-20}. **b.** Gene Ontology (GO) analysis of genes associated to c-MAF-bound regions in Day 5-activated T_H17-IL-10^+ cells. GO biological processes are ranked according to their binomial *P*-value. **c.** Graphical representation of a previously characterized (MARE_2) and a novel (IL10_MAF) c-MAF binding sites at the *IL10* locus by the Integrative Genome Viewer (IGV). **d.** The 1 kb genomic region centered on the novel putative *IL10* enhancer (IL10_MAF) was aligned to an isometric genomic region centered on a c-MAF peak localized about 9 kb upstream of *Il10* in mouse T_H17 cells[1]. The core enhancer region

shown is highly conserved between human and mouse (83% identities) and includes a canonical c-MAF binding site (highlighted in yellow). **e.** The activation status of the newly identified putative *IL10* enhancer was evaluated by quantifying H3K27ac and H3K27me3 levels in Day 5-activated T_H17-IL-10^+ and T_H17-IL-10^- cells by ChIP-qPCR (mean + s.e.m.; n=2).

[1]Ciofani, M. et al. A validated regulatory network for Th17 cell specification. Cell 151, 289-303 (2012).

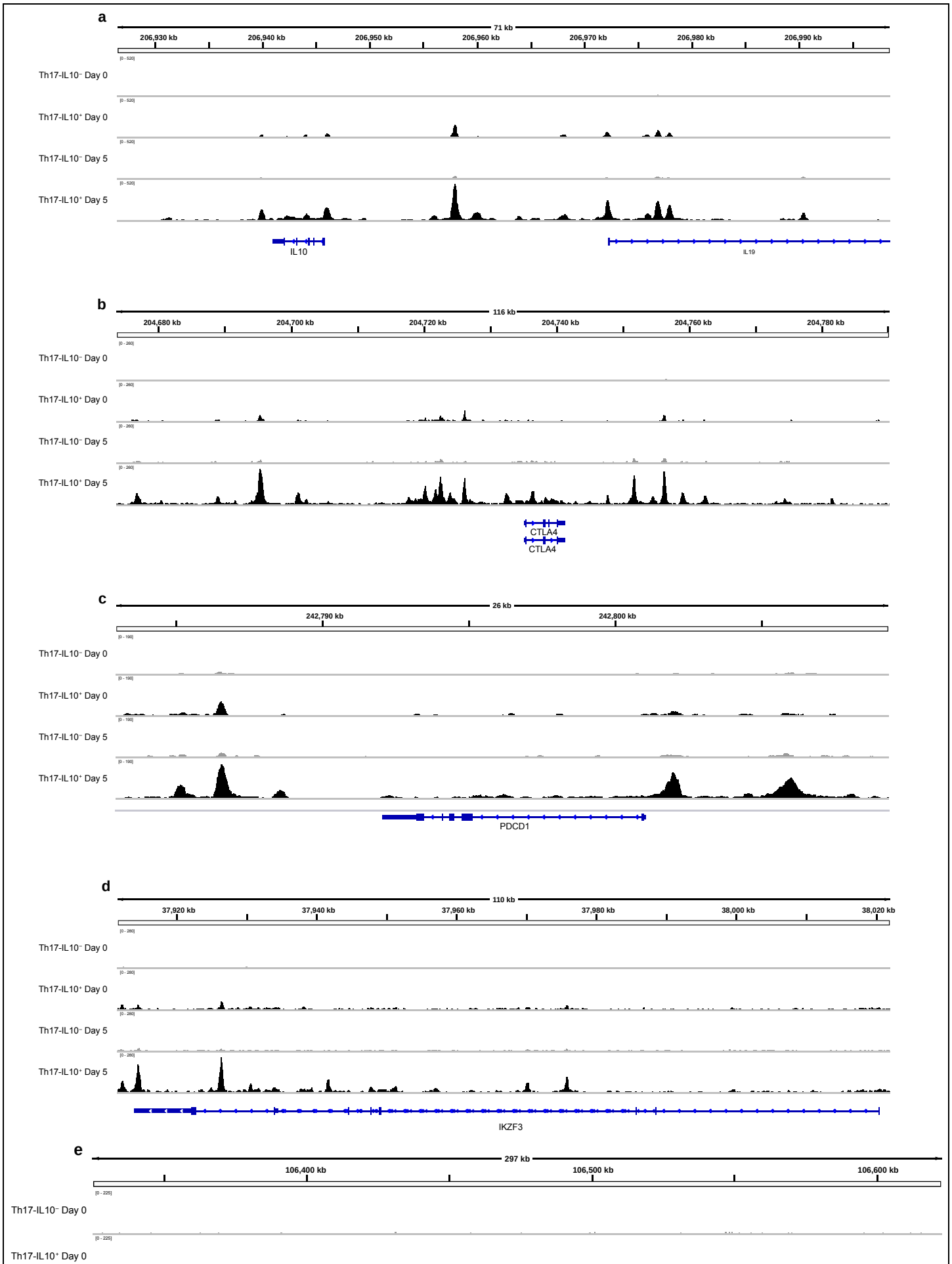
a
71 kb
206,930 kb
206,940 kb
206,950 kb
206,960 kb
206,970 kb
206,980 kb
206,990 kb
Th17-IL10⁻ Day 0
Th17-IL10⁺ Day 0
Th17-IL10⁻ Day 5
Th17-IL10⁺ Day 5
IL10
IL19
b
116 kb
204,680 kb
204,700 kb
204,720 kb
204,740 kb
204,760 kb
204,780 kb
Th17-IL10⁻ Day 0
Th17-IL10⁺ Day 0
Th17-IL10⁻ Day 5
Th17-IL10⁺ Day 5
CTLA4
CTLA4
c
26 kb
242,790 kb
242,800 kb
Th17-IL10⁻ Day 0
Th17-IL10⁺ Day 0
Th17-IL10⁻ Day 5
Th17-IL10⁺ Day 5
PDCD1
d
110 kb
37,920 kb
37,940 kb
37,960 kb
37,980 kb
38,000 kb
38,020 kb
Th17-IL10⁻ Day 0
Th17-IL10⁺ Day 0
Th17-IL10⁻ Day 5
Th17-IL10⁺ Day 5
IKZF3
e
297 kb
106,400 kb
106,500 kb
106,600 kb
Th17-IL10⁻ Day 0
Th17-IL10⁺ Day 0

1

Supplementary Figure 6
Examples of c-MAF binding to immunoregulatory and tissue-residency genes loci
a-g. Graphical representation of c-MAF binding profiles at the locus of the indicated genes using the Integrative Genome Viewer (IGV).

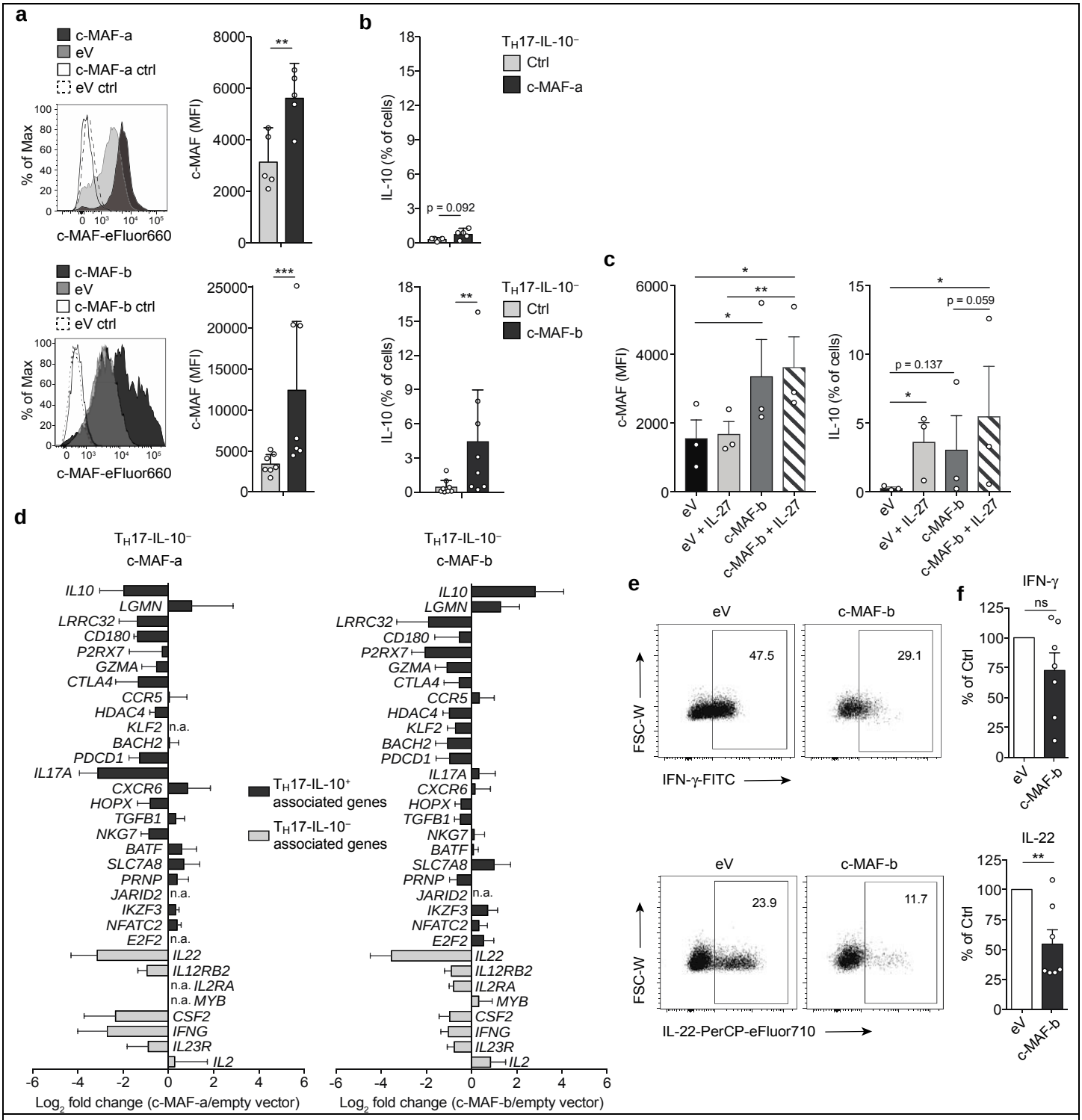

Supplementary Figure 7

c-MAF is partially sufficient to induce IL-10 expression and repress proinflammatory genes transcription in T_H17-IL-10⁻ cells

a. c-MAF isoform a (upper panels) and isoform b (lower panels) ectopic expression in Day 5-activated T_H17-IL-10⁻ cells as measured by intracellular staining; representative plots (left panels) and combined results (right panels) are displayed. **b.** IL-10 production secondary to c-MAF ectopic expression in the same cells as determined by intracellular staining. Data are represented as mean + 95%

c.i. (isoform a: n = 5, isoform b: n = 7). **c.** Expression of c-MAF and IL-10 in T_H17-IL10$^-$ cells upon ectopic expression of c-MAF isoform b. Control (empty vector) cells and c-MAF-b (c-MAF isoform b) expressing T_H17-IL10$^-$ cells were polyclonally stimulated with or without IL-27 (25 ng/ml) and c-MAF and IL-10 expression was measured in Day 5-activated cells by flow cytometry, after 5 h stimulation with PMA+I (mean + s.e.m.; n = 3). **d.** Expression of c-MAF-dependent genes in T_H17-IL10$^-$ cells upon ectopic expression of MAF isoform a (left panel, n = 4) and b (right panel, n = 6), as measured by qPCR. Black bars indicate T_H17-IL10$^+$-associated genes, grey bars indicate T_H17-IL10$^-$-associated genes. Shown is the average $\log_2$ fold change over empty vector (mean + s.e.m). n.a., not assessed. **e,f.** Representative dot plots (**e**) and cumulative data of expression of IFN-γ and IL-22 (**f**) as assessed by intracellular staining of Day 5-activated T_H17-IL10$^-$ cells following ectopic expression of MAF isoform b or control empty vector (eV). Data are expressed as percentage over empty vector and represent the mean + s.e.m. (n = 7), with each dot indicating a T cell clone pool from independent experiments. $^{**}P < 0.01$; $^{***}P < 0.001$, as determined by ratio paired *t* test (**a-c**) and paired *t* test (**f**).

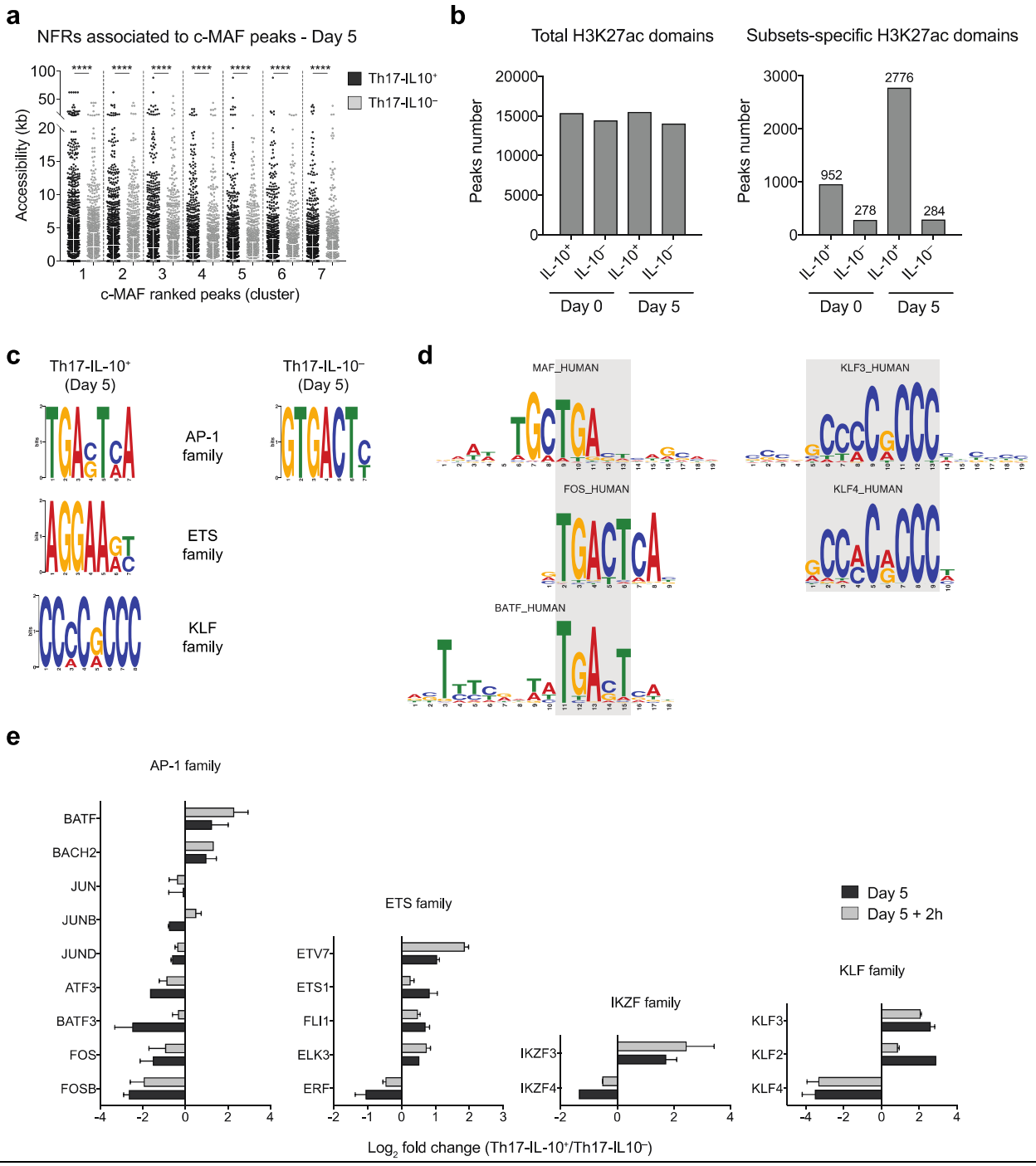

Supplementary Figure 8

Potential cooperative and antagonistic binding of transcription factors in T_H17-IL-10$^+$ and T_H17-IL-10$^-$ cells

a. c-MAF peaks from Day 5-activated T_H17-IL-10$^+$ cells were ranked according to the fold enrichment over the input, corrected for *P*-value, and clustered in bins of 1000 peaks (cluster 7 is made of 778 peaks). c-MAF peaks-associated nucleosome-free regions (NFRs) in the same cells were identified from H3K27ac ChIP-seq data and their size was compared to the corresponding NFRs in Day 5-activated T_H17-IL-10$^-$ cells. If a NFR was not detected, the size was reported as 0. Each dot in (a) represents a NFR and the white lines indicate median and interquartile ranges. *P*-values are obtained by Wilcoxon matched-pairs signed rank test. **b.** Number of total H3K27ac peaks (left panel) identified in Day 0 and Day 5 T_H17-IL-10$^+$ and T_H17-IL-10$^-$ cells, as assessed by ChIP-seq (MACS *P*-value

≤ 10 x 10^{-10}, FDR ≤ 5% and fold enrichment ≥ 5). Subset-specific H3K27ac peaks (right panel) were identified, among the total ones, as H3K27ac peaks that were specifically enriched (MACS *P*-value ≤ 10 x 10^{-6} and fold enrichment ≥ 3) in the indicated population. Multiple H3K27ac peaks residing within 1 kb were collapsed into a single domain. **c.** Position weight matrices (PWMs) of DNA enriched motives identified in NFRs associated to recently-activated T_H17-IL-10^+-specific and T_H17-IL-10^--specific H3K27ac domains. **d.** Consensus PWMs of the indicated transcription factors were downloaded from the Hocomoco v.11 database[2]. Overlapping nucleotides in consensus motifs are highlighted by a light grey box in background **e.** Gene expression profile of the indicated transcription factors in Day 5-activated T_H17-IL-10^+ and T_H17-IL-10^- cells was obtained from RNA-seq data (Fig. 4).

[2]Kulakovskiy, I.V. et al. HOCOMOCO: towards a complete collection of transcription factor binding models for human and mouse via large-scale ChIP-Seq analysis. Nucleic Acids Res 46, D252-D259 (2018).